TWELFTH EUROPEAN ROTORCRAFT FORUM

Paper No. 54

THE MODEL INVERSE AS AN ELEMENT OF A MANOEUVRE DEMAND SYSTEM FOR HELICOPTERS

H. Leyendecker

Deutsche Forschungs- und Versuchsanstalt
für Luft- und Raumfahrt

Braunschweig, F. R. Germany

September 22 - 25, 1986

Garmisch-Partenkirchen
Federal Republic of Germany

Deutsche Gesellschaft für Luft- und Raumfahrt e. V. (DGLR)
Godesberger Allee 70, D-5300 Bonn 2, F.R.G.

The question is, therefore, whether it is possible to develop the necessary control variable profiles from the command inputs by utilizing the knowledge of the control behaviour of the plant. This control procedure would relieve the load on the inner feedback loops, since, from the control theory approach, control could also take place without return difference. Figure 1 shows the general structure of the control system. This paper describes the design of the dynamic feedforward open-loop control system as the essential element of the manoeuvre demand system. However, since the model behaviour and the real system behaviour usually differ, and since the plant is subject to external disturbances, it is not generally possible to omit the inner control loops.

2. Feedforward open-loop control system

As with the well known observer structure, a model of the plant again forms an essential element of the overall feedforward control structure. As shown in Figure 2, the model $S_M=(A_M, B_M, C_M)$ and the plant $S=(A, B, C)$ are driven with the same control vector u_M. If the model S_M and the plant S match, i.e.

$$(3) \qquad \begin{aligned} A_M &= A \\ B_M &= B \\ C_M &= C, \end{aligned}$$

both the two corresponding outputs y_M and y and the associated system states x_M and x are identical. In other words, the state vector of the plant is simulated in the feedforward open-loop control system.

From the theoretical point of view, this means that the feedforward control system can be designed independently of the inner control loops of the plant, as expressed in Figure 2 by the use of the two controller matrices R_A and R_Z. Any desired eigendynamics can be set for the plant with the aid of the inner control loops without having to change anything in the feedforward control system in comparison with the uncontrolled plant. Command response and eigendynamics can be designed independently of each other.

The objective of the feedforward open-loop control system is to establish the simplest possible relationship between the command vector w and the output vector y_M of the model. By far the most important requirement is that the outputs can be decoupled and controlled independently of each other. In other words, when a command variable is changed, only the associated output should respond, whereas the remaining controlled outputs should not change. Falb/Wolovich/1/ examined the question whether such decoupling is fundamentally possible for a linear system as per Eq. (1) with state vector feedback as per Figure 2. If a decoupling solution G^*, F^* is to be obtained for the system $S_M = (A_M, B_M, C_M)$, the following condition must be fulfilled:

$$(4)\qquad \det(B^*)=\det\begin{vmatrix} & & d_1 \\ C_{M_1} & A_M & B_M \\ & & d_2 \\ C_{M_2} & A_M & B_M \\ \cdot & \cdot & \\ \cdot & \cdot & \cdot \\ & & d_m \\ C_{M_m} & A_M & B_M \end{vmatrix} \neq 0 \quad ,$$

where C_{M_i} denotes the i-th row of C_M and the integers $d_1, d_2, \ldots, d_m$ are given by

$$(5)\qquad d_i = \min \left\{ j : C_{M_i} \cdot A_M^j \cdot B_M \neq 0,\ j = 0, 1, \ldots, n-1 \right\} .$$

For the manoeuvre demand system a special solution for the decoupling pair G^*, F^* is chosen. The output vector y_M is to be related to the input vector w as follows.

$$(6)\qquad y_{M_i}^{d_i+1} = w_i \qquad i=1, 2, \ldots, m$$

Eq. (6) describes a so-called integrator decoupled system.

The special relationship of Eq. (6) implies that the pair G^*, F^* must be of the form

$$(7)\qquad F^* = -B^{*-1} A^*$$

$$G^* = B^{*-1} ,$$

where

$$(8)\qquad A^* = \begin{vmatrix} & d_1+1 \\ C_{M_1} & A_M \\ & d_2+1 \\ C_{M_2} & A_M \\ \cdot & \cdot \\ \cdot & \cdot \\ & d_m+1 \\ C_{M_m} & A_M \end{vmatrix}$$

Assuming the ideal case, i.e. the dynamic responses of the model $S_M = (A_M, B_M, C_M)$ and the plant $S = (A, B, C)$ match, the overall dynamic system behaviour of the plant cascaded with the dynamic feedforward open-loop control system is described by Eq. (9).

$$(9) \qquad y_i^{d_i+1} = w_i \qquad i=1, 2, \ldots, m$$

Consequently, the dynamic feedforward open-loop control system with the input w_i and the output u_M represents a special form of the inverse of the model of the plant, which can be referred to as the d_i-integral right inverse of the system $S_M = (A_M, B_M, C_M)$. If this right inverse is used as feedforward control system, there is a direct proportional relationship between the highest derivative $y_i^{d_i+1}$ of the controlled output variable and the input w_i. The system cannot possibly respond more quickly, since the control vector u is activated as soon as the command variable w_i is changed. The command model stimulated in a manoeuvre demand system by the pilot input vector w_p, must be designed in such a way that the (d_i+1)th derivatives of the output variables to be controlled are generated as continuous signals. These, in turn, drive the feedforward open-loop control system, from which the control vector u_M is computed as input to the real system S.

An important indication of the dynamics which can be selected for the command model can be obtained from the eigenvalues of the characteristic equation of the feedforward open-loop control system

$$(10) \qquad \det\ (I_n\, s - B_M\, F^* - A_M) = 0.$$

Equation (10) essentially has

$$(11) \qquad \sum_{i=1}^{m} (d_i + 1) = d_S \leq n$$

poles in the origin of the Gauss-plane. In the case of $d_S < n$, the remaining poles may lie outside the origin. If the system S_M has poles within the right half plane, these poles must be compensated for in the command model by corresponding numerator zeros. Otherwise the control variables would run up against its bounds, despite a restricted and initially apparently safe command function.

3. Manoeuvre demand system for the Bo 105 helicopter

Figure 3 shows how the control system of a helicopter has developed into a full fly-by-wire system without mechanical connection between

joystick and control variables. Only FBW technology, including the use of a digital computer, makes it possible to implement complex control algorithms as they were presented in Chapter 2. The control theory considerations presented in Chapter 2 are now to be implemented in a manoeuvre demand system for the Bo 105 helicopter (Figure 4).

The associated control concept foresees the pilot commanding decoupled reactions of the helicopter by means of the four traditional control elements. The collective pitch lever deflection δ_{op} corresponds to a vertical acceleration command, the longitudinal stick deflection δ_{xp} to a pitch rate command, the lateral stick deflection δ_{yp} to a roll rate command and the pedal δ_{zp} to a yaw rate command.

On a helicopter, all degress of freedom are coupled dynamically via the aerodynamics of the rotor to a far greater extent than on a fixed-wing aircraft. Longitudinal and lateral motion cannot be separated so easily, meaning that control theory results obtained with the aid of such simplifications must be considered much more critically. It is, therefore, an obvious step to base control investigations on the complete system of motion equations.

The n-dimensional state vector (n = 8)

$$x_M = | V_x, V_y, V_z, p, q, r, \Phi, \Theta |^T \tag{12}$$

and the m-dimensional control variable vector (m = 4)

$$u_M = | \delta_o, \delta_y, \delta_x, \delta_z |^T \tag{13}$$

are defined in accordance with Eq. (1),
where

δ_o = collective actuator position

δ_y = lateral cyclic actuator position

δ_x = longitudinal cyclic actuator position

δ_z = pedal actuator position.

In accordance with the selected assignments of control deflections and the output variables intended to respond in decoupled fashion, the output matrix C_M has the following form:

$$(14) \qquad y_M = \begin{vmatrix} V_z \\ p = \dot{\Phi} \\ q = \dot{\Theta} \\ r \end{vmatrix} = \begin{vmatrix} 0\,0\,1\,0\,0\,0\,0\,0 \\ 0\,0\,0\,1\,0\,0\,0\,0 \\ 0\,0\,0\,0\,1\,0\,0\,0 \\ 0\,0\,0\,0\,0\,1\,0\,0 \end{vmatrix} \cdot x_M$$

A check is first made whether the helicopter motion can be decoupled in the sense of the control concept expressed in Eq. (4). Since the helicopter can also be flown in decoupled fashion with 1:1 control, the check according to Eq. (4) must, of course, confirm this fact. All values of d_i, $i = 1, \ldots, m$ add up to zero. This result can also be immediately demonstrated physically: the quickest helicopter reaction to step inputs in the control variables as defined in Eq. (13) is vertical acceleration respectively rotary accelerations about the three axes can be generated.

According to Eq. (10), the characteristic equation for the feedforward open-loop control system of the Bo 105 helicopter has not only poles in the origin, but also two stable eigenvalues on the real axis, as shown by numerical calculations. The stable eigenvalues indicate that the command models in Figure 2 may be pure lag elements.

Since, for purely anthropotechnical reasons, the pilot cannot be expected to command rotary accelerations about the three axes proportional to his command inputs, first-order systems are used as command models in these three input channels, as shown for the example of the pitch rate input in Figure 5. The pitch rate command $\dot{\Theta}_c^* = \delta_{xp}$ of the pilot is quasi-differentiated by the lag element to generate the $\ddot{\Theta}_c$-signal, which drives the dynamic feedforward open-loop control system as $\dot{w}_3$-signal.

As long as the capacity of the control variables is not exceeded, the plant can follow this $\ddot{\Theta}_c$-signal and thereby the $\dot{\Theta}_c$-, Θ_c-signals of Figure 5 in decoupled fashion.

Figure 6 shows the simulation results for the $\dot{\Theta}_c$- and $\ddot{H}_c$- commands. The control variables demand required is computed by the feedforward control system, meaning that the helicopter follows the command inputs in decoupled fashion and without return differences. The inner loops only become active if the model S_M does not match the plant, or if the helicopter is exposed to external disturbances.

The eigendynamics of the Bo 105 helicopter are largely determined by an unstable complex conjugate root pair. An example of the effects of this instability is shown in Figure 7. The trimmed helicopter could only be left to its own devices for about 150 s. Then the pilot inputs are required in order to return the dangerous build-up of the state variables to the normal flight range. As shown in Figure 8, this unstable root pair can be shifted into a stable range merely by means of two relatively simple inner loops, namely by feedback of the pitch angle and pitch rate to the longitudinal cyclic. The gains are chosen to be as weak as possible, in order to minimize the control activities. Similar considerations lead to feedback loops for the remaining three control variables; these are also relatively simple, and their final gains can easily be determined in flight

tests. The command response remains largely unaffected by these inner control loops, whereas the response to disturbances is considerably improved due to the changed eigendynamics.

4. Flight tests

The DFVLR uses the Bo 105-S3 helicopter, equipped with a simplex fly-by-wire system as an experimental aircraft for testing the control algorithm developed in the preceding Chapters. The measuring equipment is based on the strap-down platform LTR 81 from Messrs. Litef, an air data computer for altitude rate and air speed and a Doppler speed sensor. The test data are transmitted to the ground via a PCM telemetry link and recorded in digital form. With the current configuration, the experimentor has 79 data channels at his disposal.

All flight tests were intentionally performed only with a linear model of the helicopter dynamics as per Eq. (1); the inner control loops operated with constant, relatively weak gains. Satisfactory results were nevertheless obtained, since the dynamic feedforward open-loop control system tended at least to compute the necessary control input profiles due to the command inputs, meaning that the inner control loops were certainly relieved of a considerable load.

5. Flight test results

Figure 9: Vertical acceleration command.
The pilot commands a vertical acceleration via the collective lever. This signal drives the feedforward open-loop control system, this in turn computing the control vector u_M, the state vector x_M and the output vector y_M. The four actuator movements are essentially determined by the feedforward control system, although the high-frequency components result from the inner control loops and improve the eigendynamics of the originally unstable plant. The vertical acceleration command has hardly no effect on the roll and pitch angles; although not controlled, the air speed changes only slightly.

Figure 10: Pitch rate command.
The pilot commands the pitch rate via a longitudinal stick movement. As already shown in Figure 5, the pilot command is differentiated and passed to the feedforward open-loop control system as input. The model $S_M = (A_M, B_M, C_M)$ obviously provides only an incomplete description of the pitch/roll coupling of the plant, meaning that the lateral motion is activated too strongly despite the feedforward control system. So the inner loops have to return the roll angle to zero during this flight phase; the feedforward control of the lateral cyclic in particular is unsatisfactory. The output variables for longitudinal motion, on the other hand, are decoupled relatively well, the commanded descent being hardly affected at all during the air speed changes between 30 m/s and 55 m/s.

Figure 11: Roll rate command.
In order to fly a coordinated turn, the pilot must set the desired roll attitude via a pulselike deflection of the lateral cyclic stick. At the same time, a control command for the yaw rate is computed in accordance with the roll attitude and air speed and passed to the feedforward control system. The altitude rate and air speed change only insignificantly during turning. A heading-hold function is active in horizontal flight. In this case, a roll rate command is computed from the course return difference and superimposed on the pilot's command. This process causes the higher-frequency roll rate commands in the first trace of Figure 11 during phases where the roll angle command of the pilot is equal to zero.

6. Conclusions

Increasing efforts have been made in recent years to transfer the status of FBW technology in fixed-wing aircraft to the helicopter sector. However, in the entire world, there are only few test aircraft equipped with an FBW system. The Bo 105-S3 helicopter enables the DFVLR to play a creative role and make important contributions towards developments in this future-oriented sector.

The concept of a manoeuvre demand system for helicopters presented in this paper and tested in flight can be seen as a first step towards practical helicopter control systems. Control engineering investigations in the entire flight envelope, from hovering and transition to high-speed forward flight must now follow. The dynamic feedforward open-loop control system as an element of a helicopter flight control system can play a major role in this respect, where non linear modelling of the plant will no doubt be necessary.

7. References

1. P. L. Falb, W. A. Wolovich — Decoupling in the Design and Synthesis of Multivariable Control Systems. IEEE Transactions on Automatic Control, Vol. AC-12, No. 6, December 1967 (pp. 651-659).

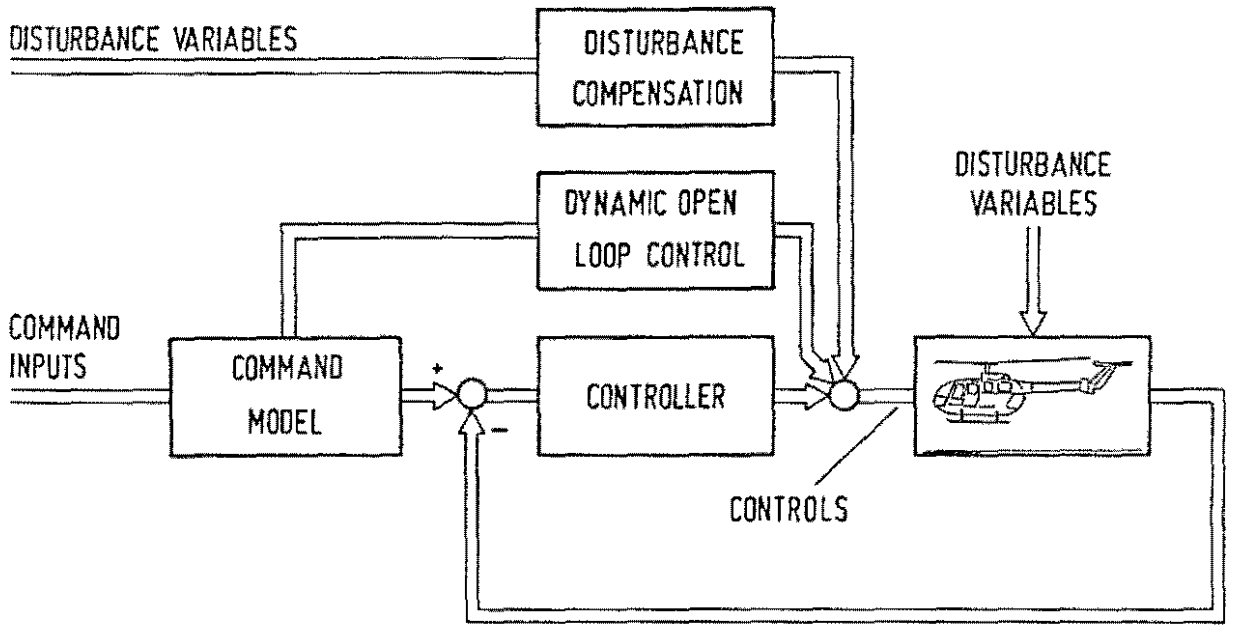

Figure 1: Block diagram of the flight control system

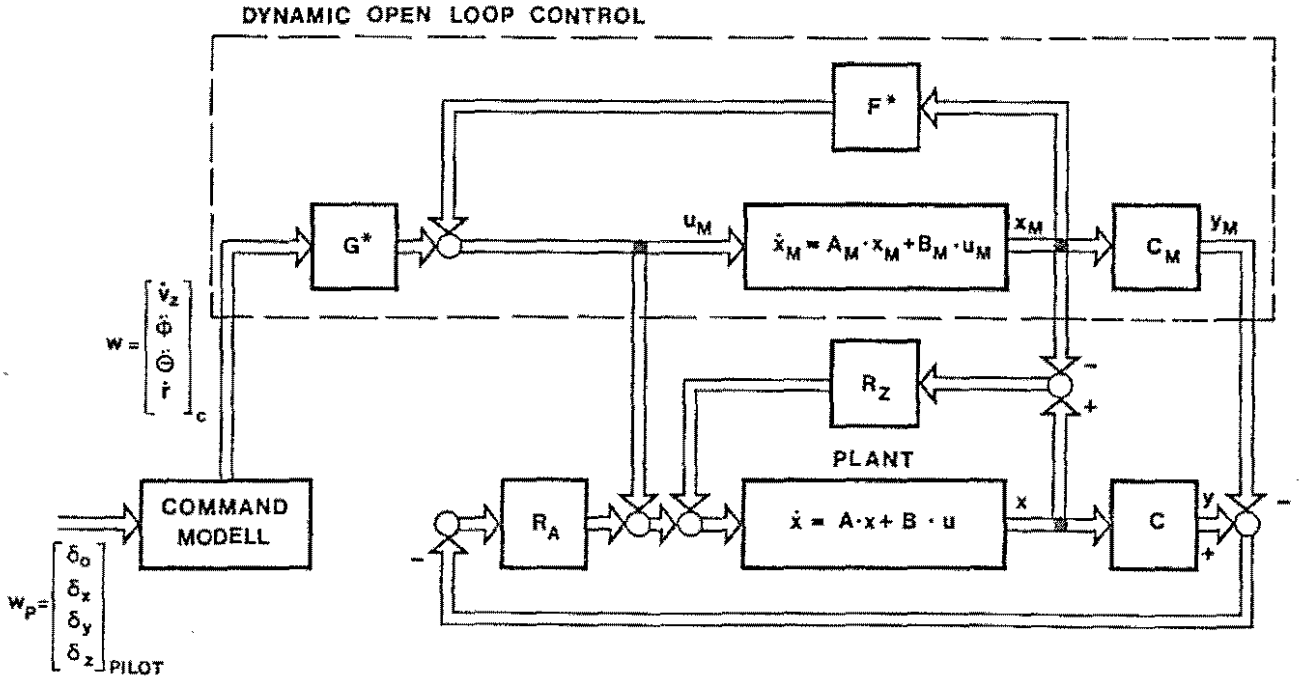

Figure 2: Functional diagram of the dynamic open loop control system

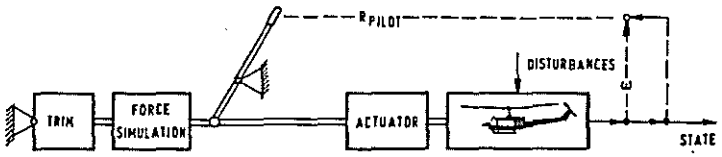

Conventional

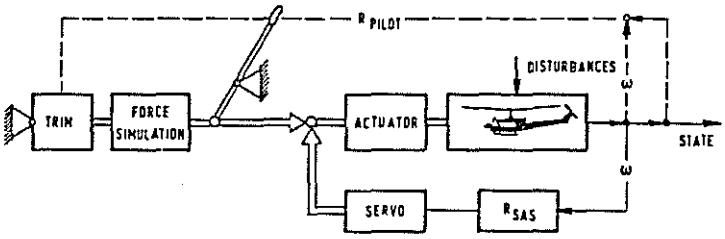

Stability augmentation system

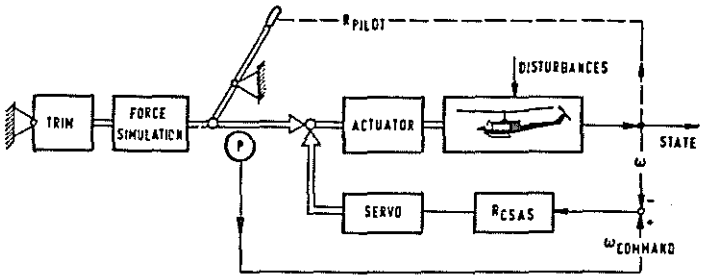

Computed stability augmentation system with limited authority

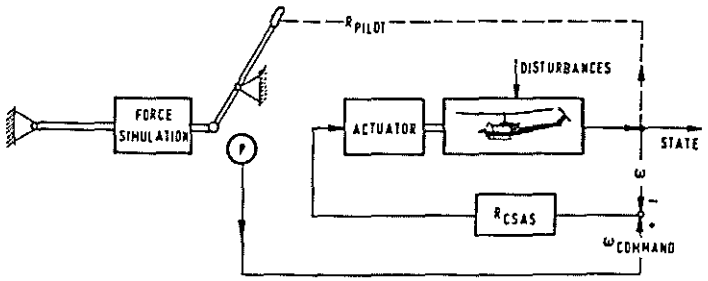

Manoeuvre demand system

Figure 3: Guidance and control concepts

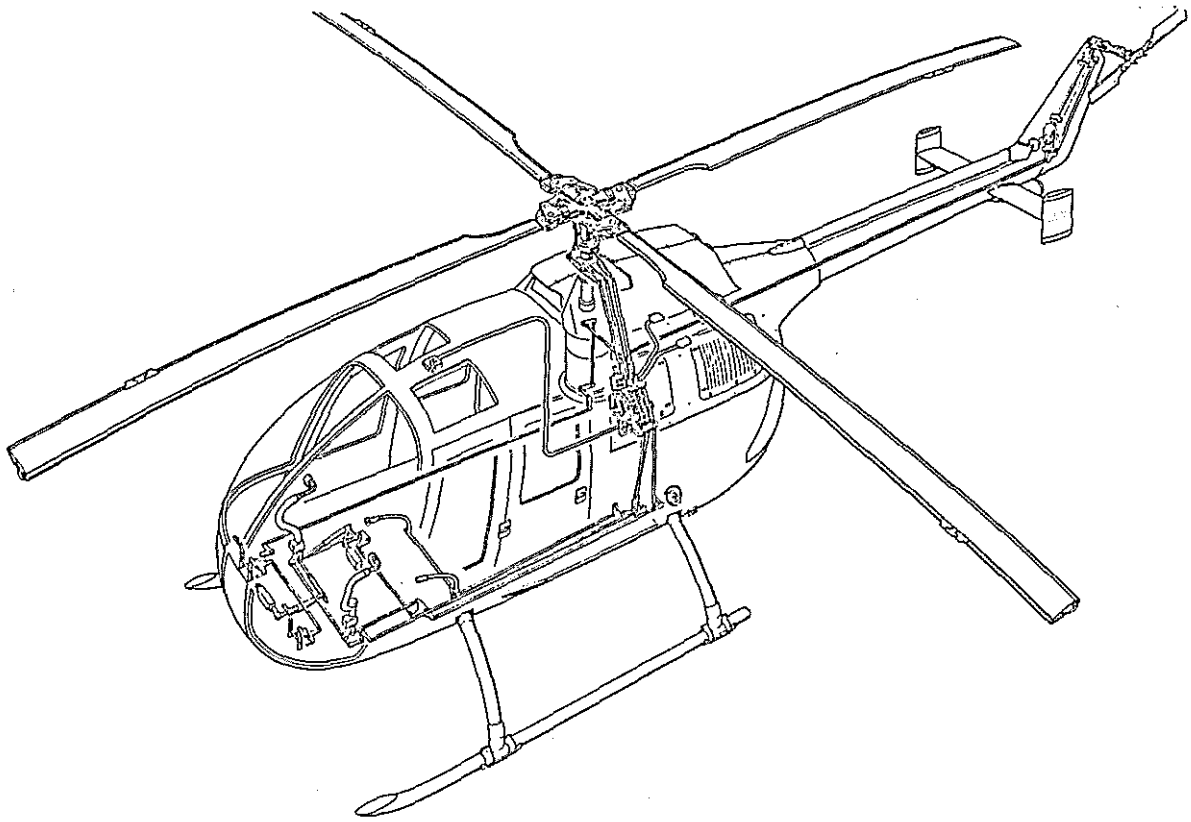

Figure 4: Helicopter BO 105

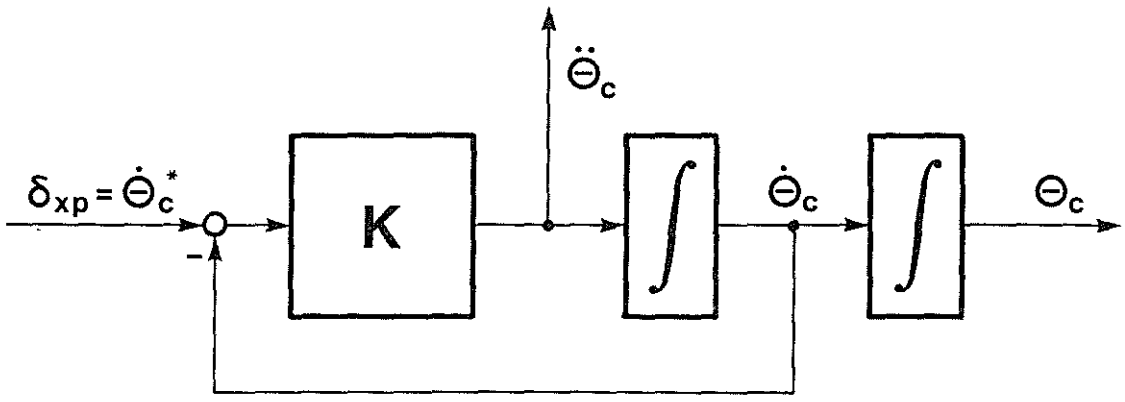

Figure 5: Command model for pitch rate

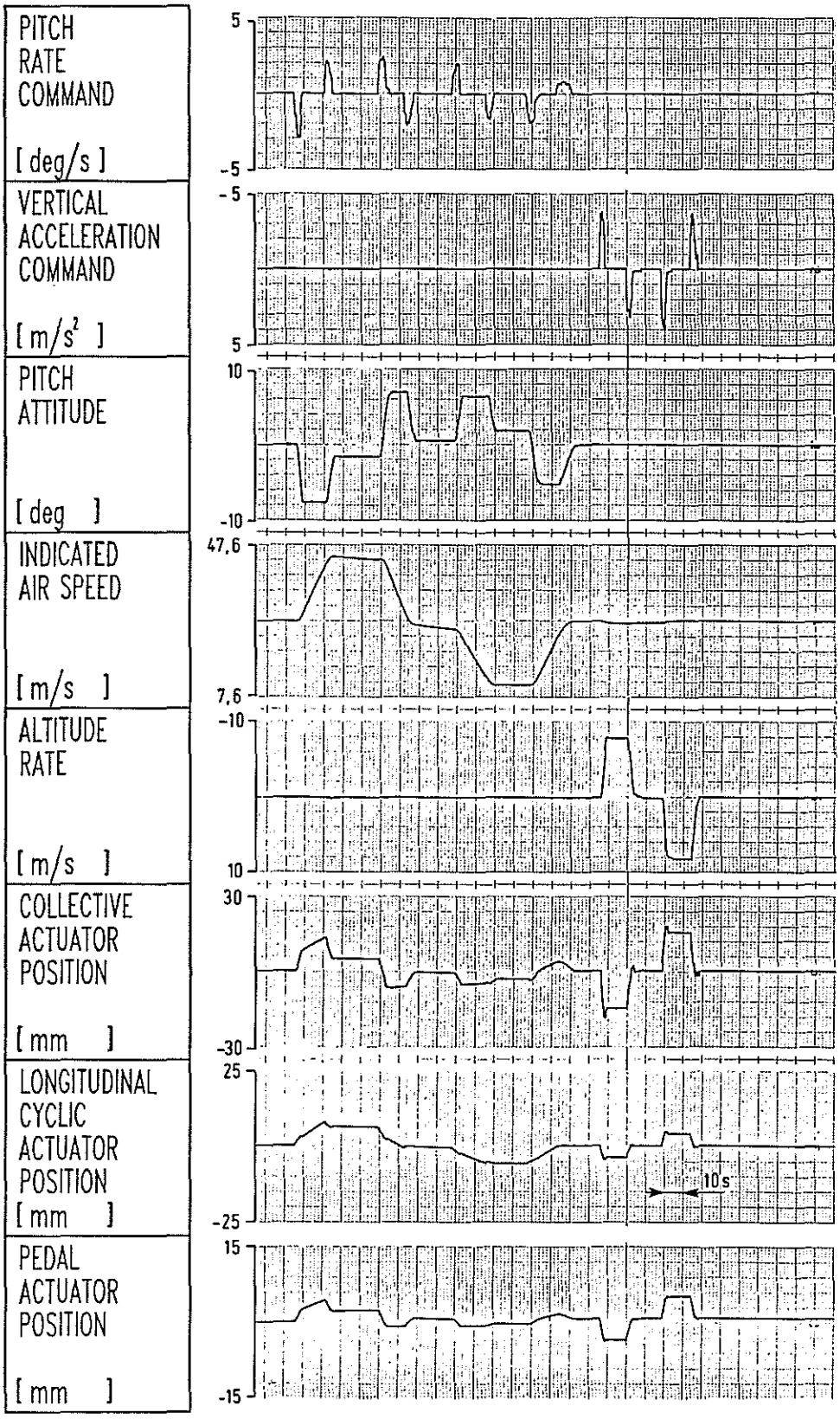

Figure 6: Simulation result of pitch rate and vertical acceleration commands (BO 105)

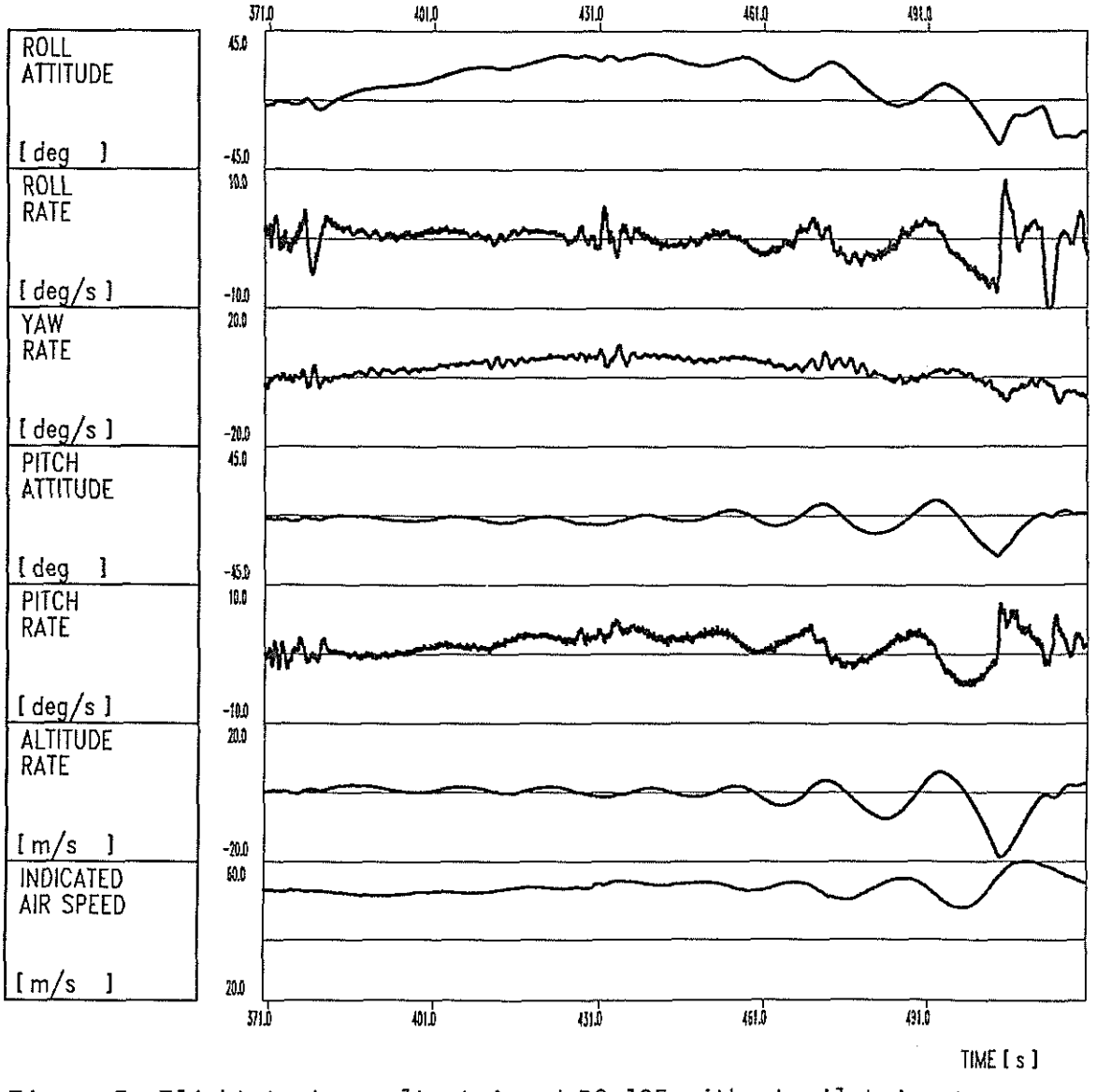

Figure 7: Flight test result, trimmed BO 105 without pilot inputs

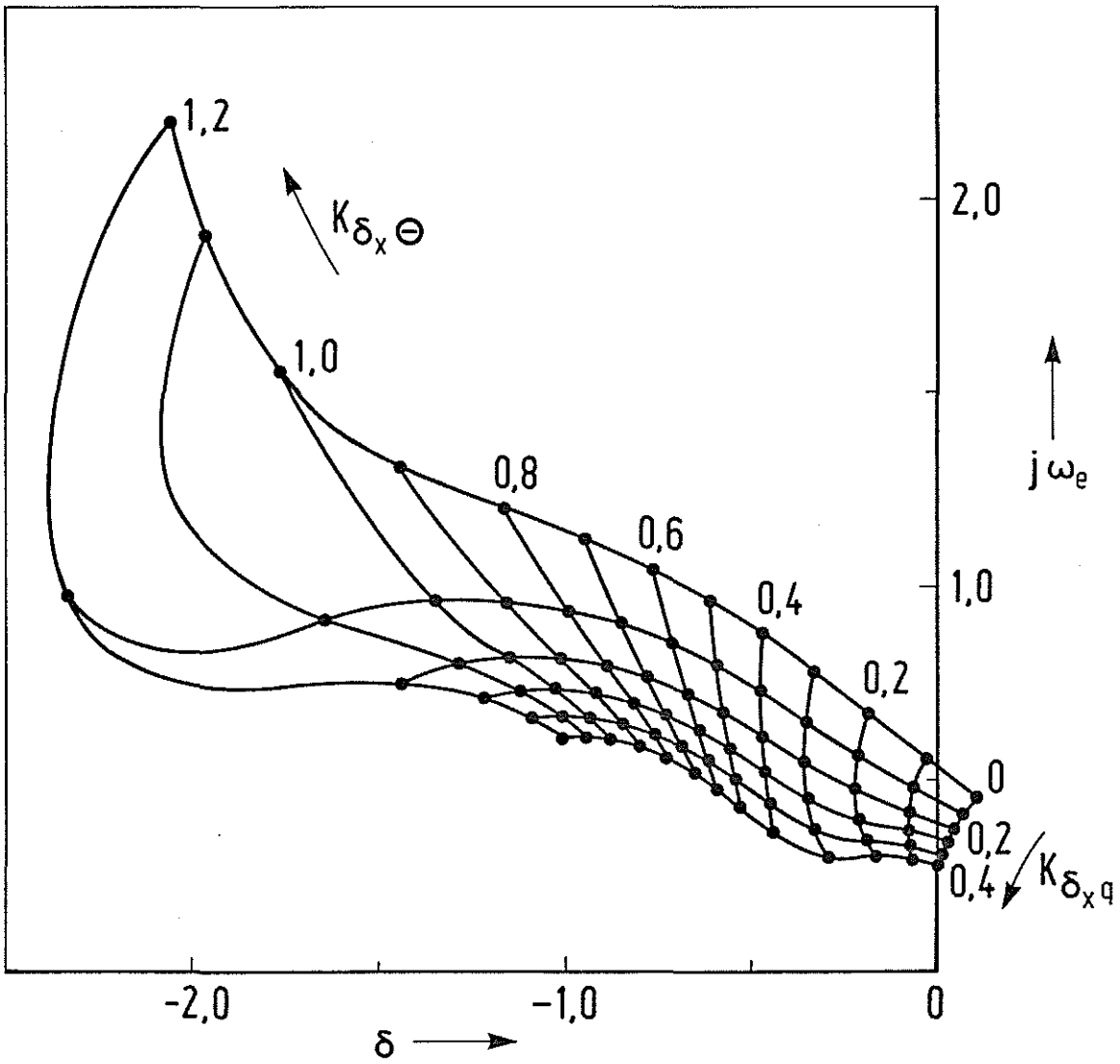

Figure 8: Root locus for pitch rate and pitch attitude feedback to longitudinal cyclic actuator (BO 105, V_o=50 m/s)

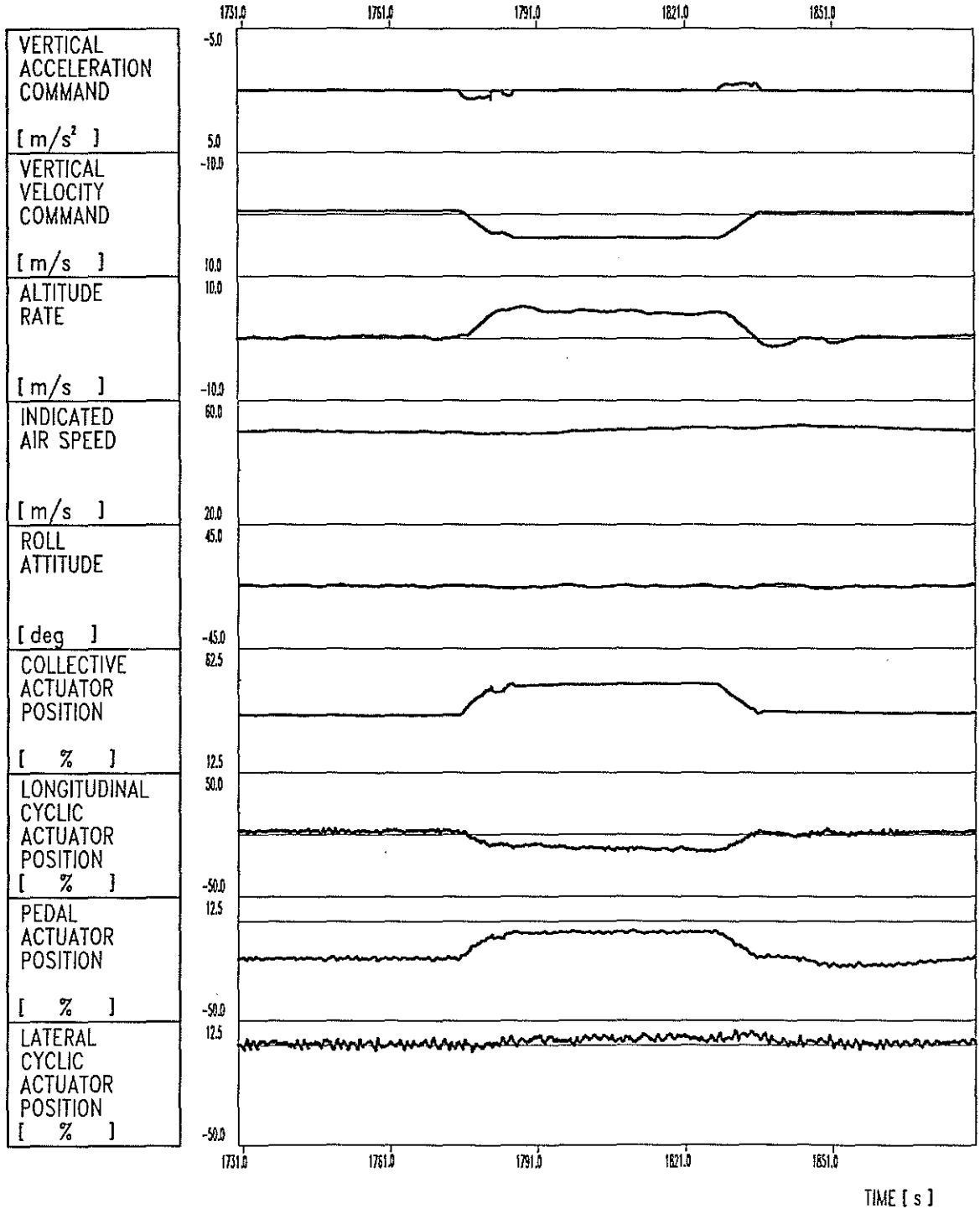

Figure 9: Flight test result with the manoeuvre demand system, vertical acceleration command

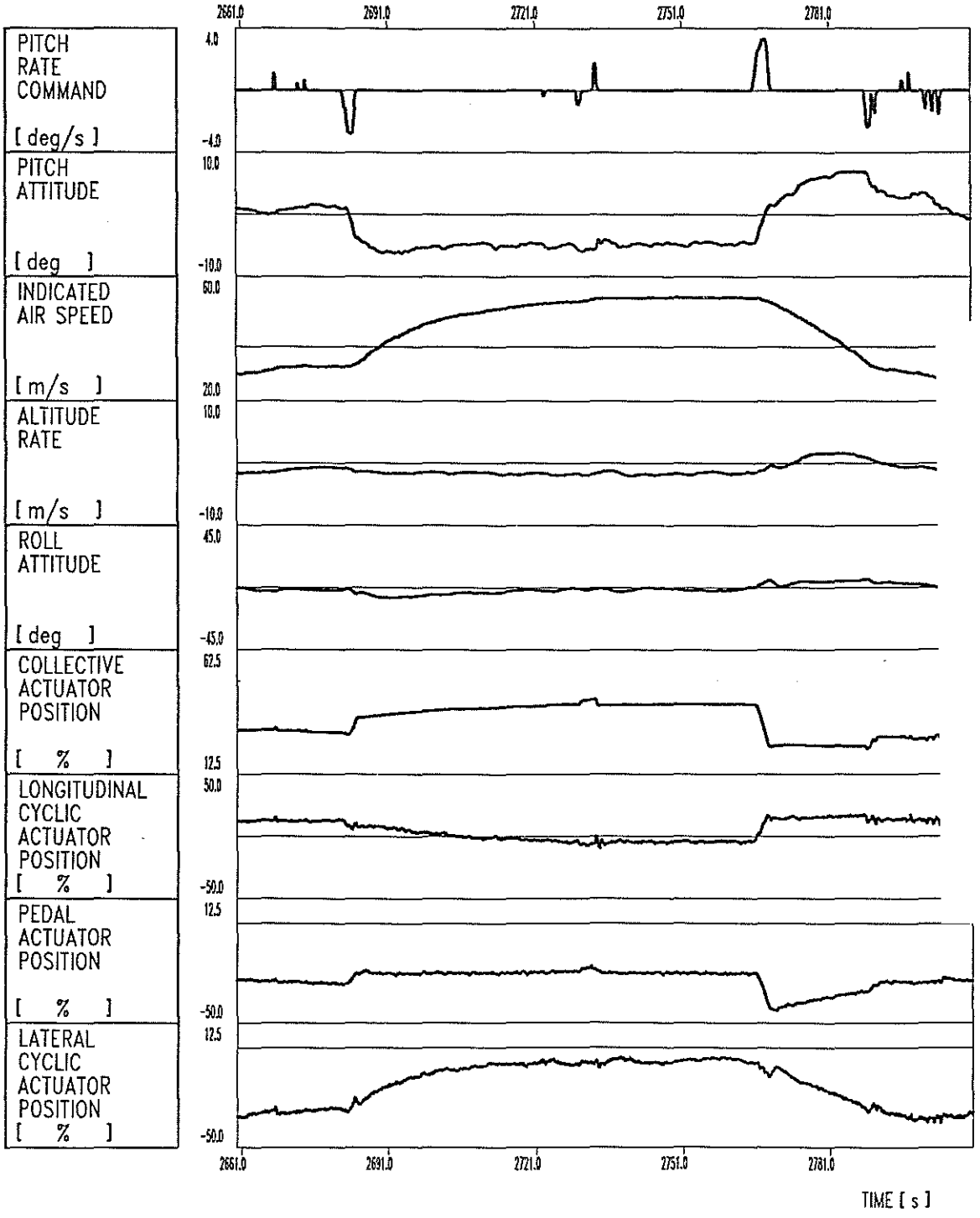

Figure 10: Flight test result with the manoeuvre demand system, pitch rate command

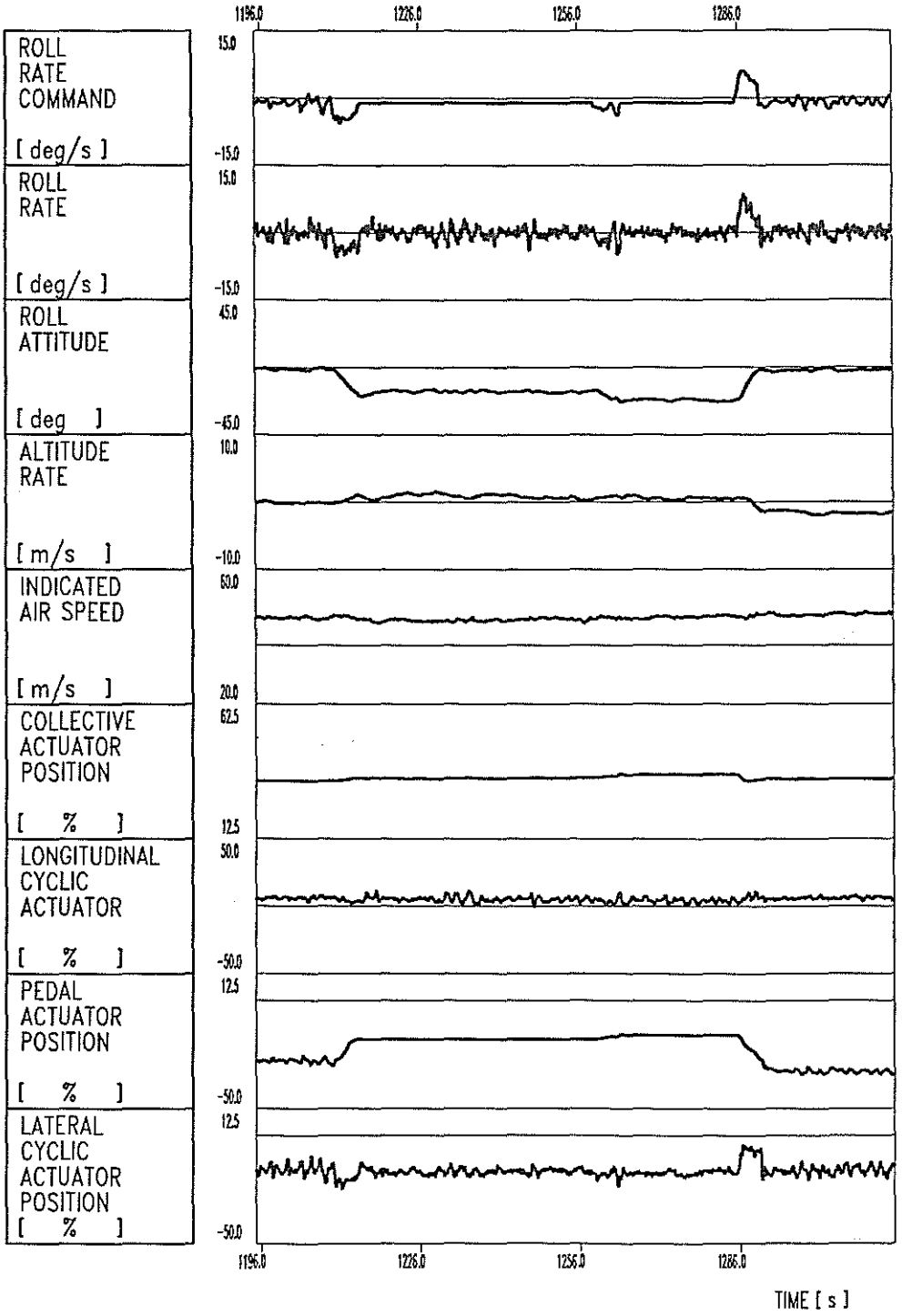

Figure 11: Flight test result with the manoeuvre demand system, roll rate command